Journal of Alloys and Compounds 509 (2011) 8130–8135

Contents lists available at ScienceDirect

Journal of Alloys and Compounds

journal homepage: www.elsevier.com/locate/jallcom

Plate-type $LiFePO_4$ nanocrystals by low temperature polyol-assisted solvothermal reaction and its electrochemical properties

Jinsub Lim [a], Donghan Kim [a], Vinod Mathew [a], Docheon Ahn [b], Jungwon Kang [a], Sung-Won Kang [a], Jaekook Kim [a,*]

[a] Department of Materials Science and Engineering, Chonnam National University (WCU), 300 Yongbongdong, Bukgu, Gwangju 500-757, South Korea
[b] Beamline Research Division, Pohang Accelerator Laboratory, Pohang 790-784, South Korea

ARTICLE INFO

Article history:
Received 7 April 2011
Received in revised form 20 May 2011
Accepted 20 May 2011
Available online 27 May 2011

Keywords:
Nanoplates
$LiFePO_4$
Lithium batteries
Electrode
Cathode

ABSTRACT

Highly nanocrystalline $LiFePO_4$ was synthesized by a solvothermal process in a polyol medium namely, diethylene glycol (DEG) without any heat-treatment as a post procedure. The synchrotron powder XRD pattern of the $LiFePO_4$ was indexed well to a pure orthorhombic system of olivine structure (space group: Pnma) with no undesirable impurities and refined fit parameters were obtained by the Rietveld refinement method using the FULLPROF program. XPS analysis revealed the divalent state of iron (Fe(II)) in the prepared sample thereby further confirming the formation of a pure olivine phase. The synthesized $LiFePO_4$ nanocrystals exhibited well dispersed plate morphologies with average length, width and thickness of 250, 200 and 20 nm, respectively. Nanoplate $LiFePO_4$ indicated initial discharge capacity of 138 mA h/g and exhibited stable capacity retention until 50 electrochemical cycles. It also appeared to reveal considerably better rate performance at enhanced C-rates because of the contribution from nano-dimensional particles when compared to that of $LiFePO_4$ synthesized by solid state method.

1. Introduction

Olivine $LiMPO_4$ (M = Fe, Mn, Ni, Co) has been identified as an excellent candidate for cathodes in rechargeable Li-ion batteries when compared to its counterparts as $LiCoO_2$, $LiNiO_2$ and $LiMn_2O_4$ because of its environmental benignity, relatively high capacity of 170 mA h/g, cost-effectiveness, non-toxicity, electrochemical and thermal stability [1]. Among the investigated olivines, particular attention has been focused on $LiFePO_4$, which has a suitably flat voltage-region (3.4 V) related to the liquid electrolyte window. However, despite these advantages, its unimpressive rate performance due to intrinsic problems of low ionic and electronic conductivities still remain a major obstacle for commercial applications. Progressive efforts to circumvent this drawback by carbon/oxides coating on particle surface [2–4], developing composites via mixing conductive materials [5–7], cation substitution [8–11], particle-size minimization [12,13], and customizing particle morphologies [14–18] have been undertaken. Especially, nanometer-sized electrodes have been intensively investigated for high energy/power density applications as the advantage of using nanometer-sized electrodes remains two-fold. Firstly, nanomaterials provide a favorable structural framework that ensures apparently shorter diffusion paths for the Li-ion to traverse from the core of the particles to the surface through the lattice thereby yielding excellent electrochemical properties [12,13]. Secondly, the large surface area of nanomaterials ensures enhanced electrode/electrolyte interfacial contact thus leading to higher charge/discharge rates and good capacity retentions.

In view of these aspects, many research groups have attempted to synthesize highly crystalline nanoparticles using various synthetic techniques under different conditions, including the solid-state method, coprecipitation in an aqueous solvent, the sol–gel method, mechanochemical activation, hydrothermal and solvothermal methods [14–17,19–26]. However, mandatory post-heat treatments are required to achieve sufficiently crystalline particles in these methods, which consequently raise procedure complexity and costs. For example, the solid state process requires repeated grinding and heat-treatment at high temperatures (500–600 °C) for several hours under an inert gas atmosphere, which in most cases, leads to detrimental particle-growth and increases complexity of the synthetic procedure and cost [19]. Dokko et al. showed that plate-type $LiFePO_4$ with large ac faces exhibiting high discharge capacity of 163 mA h/g can be synthesized by hydrothermal method at a pH value of 5.1 [14]. Saravanan et al. reported impressive rate performances of $LiFePO_4$ nanoplates wrapped by 5 nm thick uniform carbon coating at the particle boundaries by solvothermal process [17]. However, these approaches also required inevitable post-heat treatments to

* Corresponding author. Tel.: +82 62 530 1703; fax: +82 62 530 1699.
E-mail address: jaekook@chonnam.ac.kr (J. Kim).

0925-8388/$ – see front matter © 2011 Elsevier B.V. All rights reserved.
doi:10.1016/j.jallcom.2011.05.081

achieve sufficient particle crystallinity and carbonization, thereby raising procedure costs and complexities. Owing to these reasons, a cheap, safe, and simple process for preparing phase-pure $LiFePO_4$ nanoparticles with highly crystalline nature remains critical.

In the light of the above discussions, our group earlier proposed the polyol process as a new method of synthesizing $LiFePO_4$ with well-defined nanoparticles and high crystallinity, without the need of any further heating as a post treatment [27]. In this process, the polyol medium acts not only as a solvent, but also as a reducing environmental agent and stabilizer, thereby limiting particle growth and preventing agglomeration [27]. In fact, our earlier study appear to indicate that the type of polyol medium used in the synthetic process considerably influences the crystalline nature of the final nanopowders and one of the main possibilities for such an observed trend may probably be due to the differences in the respective boiling points of each polyol [28]. In other words, the prepared nano $LiFePO_4$ in ethylene (EG) or diethylene (DEG) glycols which possesses apparently lower boiling points of 197 and 245 °C, respectively, than triethylene (TEG) or tetraethylene (TTEG) glycols exhibited poor crystalline phases. Therefore, we considered the apparently lower boiling point polyol medium namely, DEG for the production of highly nanocrystalline particles with the application of high pressure as a crucial factor at temperatures as low as 200 °C. Hence we adopted the solvothermal method as a process for synthesizing $LiFePO_4$ nanoparticles with high crystallinity at apparently lower synthetic temperatures. The solvothermal process is especially advantageous for synthesizing $LiFePO_4$ due to its reducing conditions, quick and simple synthesis at low energy and cost. In this work, we report the synthesis of a highly crystalline and nanostructured olivine $LiFePO_4$ by the solvothermal method employing a polyol medium, namely, DEG at low temperatures. The physical properties and electrochemical performances of the obtained nanosized $LiFePO_4$ were also investigated.

2. Experimental procedures

$LiFePO_4$ nanocrystals were synthesized by the solvothermal method in a Teflon-lined stainless steel bomb. $(C_2H_3O_2)_2Fe$ (99.995%, SIGMA ALDRICH), H_3PO_4 (above 85%, DAEJUNG Chemicals & Metals Co., Ltd), and $CH_3COOLi{\cdot}2H_2O$ (GR, Junsei Chemical Co., Ltd) were added to $(HOCH_2CH_2)_2O$ (99%, DAEJUNG Chemicals & Metals Co., Ltd) in the molar ratio 1:1:1 (Li:Fe:P) and stirred for about 30 min at room temperature. The mixed solution was sealed in a 40 ml-Teflon-lined bomb and heated at 200 °C for 16 h. The resulting solution containing precipitates was washed several times with acetone and methanol in order to remove the remaining organic compounds. The obtained precipitate was then separated by filtering using ceramic membrane funnels and vacuum dried at 120 °C for 12 h before further characterizations. As a counterpart sample, $LiFePO_4$ was prepared by conventional solid state reaction from Li_2CO_3 (Extra Pure, Yakuri Pure Chemicals Co., Ltd), $FeC_2O_4{\cdot}2H_2O$ (99%, ALDRICH), and $(NH_4)_2HPO_4$ (GR, JUNSEI, 99%) in a stoichiometric molar ratio (1:1:1) and the synthesis details are given elsewhere [19].

The synchrotron powder XRD pattern of the sample was obtained using the beam line BL-8C2 of the Pohang Accelerator laboratory, Korea. The XRD pattern was fitted by the whole-pattern profile matching method in order to determine accurately the unit cell parameters of the sample, and refined by Rietveld analysis using the FULLPROF program. XPS analysis was performed on the $LiFePO_4$ samples to determine the oxidation state of Fe. The particle morphology and size were observed by field emission-scanning electron microscopy (FE-SEM) and high resolution transmission electron microscopy (HR-TEM). The electrochemical properties of $LiFePO_4$ sample were evaluated with lithium metal as the reference electrode. The active material was mixed with 30 wt% of conductive carbon (Ketjen black) and TAB (Teflonized Acethylene Black) was used as a binder. The mixture was pressed onto a stainless steel mesh and vacuum dried at 120 °C for 12 h, thus forming the cathode. A 2032 coin type cell consisting of the cathode and lithium metal anode separated by a polymer membrane together with glass fiber was fabricated in an Ar-filled glove box and aged for 12 h before the electrochemical measurements. The electrolyte employed was a 1:1 mixture of ethylene carbonate (EC) and dimethylcarbonate (DMC) containing 1 M $LiPF_6$.

3. Results and discussion

The synchrotron powder XRD pattern of the $LiFePO_4$ nanoparticle prepared by solvothermal reaction was fitted by the whole-pattern profile matching method and all the peaks were indexed to the orthorhombic olivine-type system and designated to the space group (Pnma), as shown in Fig. 1. The refined parameters and reliability factors obtained by Rietveld analysis using the FULLPROF program are summarized in Table 1. The unit cell parameters for the orthorhombic cell were evaluated to be $a = 10.3040$, $b = 5.9829$, and $c = 4.6950$ Å and these values are slightly lower than those reported in the literature [1] most probably due to the highly nanocrystalline sample characteristics. Interestingly, the unit cell volume of the solvothermal sample was determined to be 289.436 $Å^3$ which is slightly lower than that calculated for the high temperature (700 °C) solid-state $LiFePO_4$ (291.3 $Å^3$) [1] but is comparable to that of the low temperature hydrothermal sample obtained by Chen and Whittingham [29]. Their study reports that the value of the cell volume is associated with a measure of the iron disorder in $LiFePO_4$ thereby indicating the degree of electrochemical stability in the corresponding sample. The proximity in the values of the cell volume for $LiFePO_4$ prepared in the present study to that of the standard solid-state sample clearly suggests that the iron disorder remains considerably low and

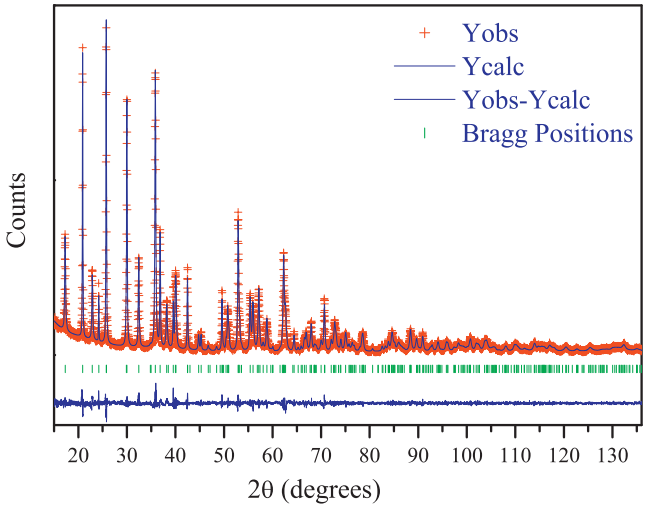

Fig. 1. Synchrotron X-ray powder diffraction spectra of nanoplate $LiFePO_4$ prepared by solvothermal reaction and comparison with the observed, calculated and differential curves.

Table 1
Rietveld refinement results of the nanoplate $LiFePO_4$ powder sample using synchrotron X-ray diffraction data.

			$LiFePO_4$		
Space group			*Pnma*		
a (Å)			10.3040(1)		
b (Å)			5.98299(8)		
c (Å)			4.69508(5)		
Atom	Site	Wyckoff positions	B_{iso} ($Å^2$)		
Li	4a	0	0	0	1[a]
Fe	4c	0.2816(2)	0.25	0.9758(6)	0.56(4)
P	4c	0.0965(3)	0.25	0.4211(7)	0.47(9)
O (1)	4c	0.0968(9)	0.25	0.739(1)	0.69(5)
O (2)	4c	0.456(1)	0.25	0.209(1)	0.69(5)
O (3)	8d	0.1691(7)	0.046(1)	0.2805(7)	0.69(5)

Angular range	$2\theta_{min} = 15°$, $2\theta_{max} = 136°$
Synchrotron X-ray radiation wavelength (Å)	1.5490
Preferred orientation correction	None
Reliability factors	$R_p = 7.5\%$, $R_{wp} = 9.82\%$, $R_{exp} = 7.33\%$, $R_B = 4.71\%$, $S = 1.33$

[a] Fixed parameter.

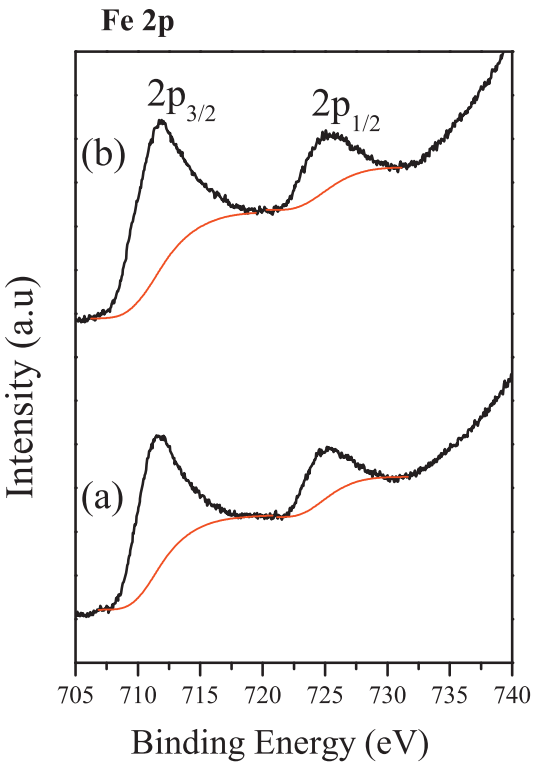

Fig. 2. XPS spectra for iron ions in $LiFePO_4$ samples synthesized by (a) solid state reaction and (b) solvothermal method.

is most probably attributed to a well ordered internal structure in the synthesized olivine sample. Moreover, these results indicate that low temperature solvothermal techniques are capable to produce electrochemically potential nanoelectrode materials. Therefore, the XRD results confirmed that the solvothermal process could successfully and effectively produce phase pure $LiFePO_4$ with no undesirable impurities such as Li_3PO_4 or transition metal compounds and requiring no further heat treatment as a post step thereby significantly reducing reaction time-durations. Additionally, this also indicates that highly nanocrystalline $LiFePO_4$ can be successfully synthesized by the solvothermal method at temperatures as low as 200 °C while it tends to be impossible to prepare such crystalline nanoparticles using the same polyol medium at similar temperatures by the polyol refluxing process [27].

XPS analysis revealed that Fe $2p_{3/2}$ peaks occurred at binding energy values of 711.4 and 711.5 eV, as shown in Fig. 2, for the solid-state and solvothermal samples, respectively. The obtained binding energies are in proximity to that of Fe(II) state [30]. This result clearly demonstrates that Fe exists in the divalent state in the solvothermal sample thereby indicating the dependability on low temperature synthesis to obtain phase pure olivine samples.

FE-SEM was used to elucidate on the particle size and morphology of the prepared olivine samples. Fig. 3(a) shows well-defined and mono-dispersed plate-type $LiFePO_4$ nanoparticles with average length, width and thickness of 250, 200 and 20 nm, respectively, while the sample prepared by solid state reaction possessed irregular morphologies with poor size distribution as evident from Fig. 3(b). The nanoplate morphology has particular advantages associated with ion-transport kinetics and is discussed in detail later. In addition, the nano-plate type morphology tends to improve the overall tap density thereby addressing an important and useful aspect for commercialization.

In order to identify the crystallographic characteristics of the well-defined $LiFePO_4$ nanoplates, TEM was used at low and high magnification with electron diffraction. Fig. 4(a) shows the low magnification FE-TEM image and the inset image corresponds to the selected area electron diffraction (SAED) spot pattern indicating the crystallographic orientation in a primary plate-type nanoparticle. The facets of the nano-plate was determined to be (0 0 1), (0 1 0) and (1 0 0), as observed from the SAED pattern and clearly indicated the growth of the nanocrystals along the [1 0 0] and [0 1 0] directions, as shown in Fig. 4(a). Fig. 4(b) shows the interplanar distances calculated using a high magnification FE-TEM image and the crystallographic simulation of olivine-structured $LiFePO_4$ projected on the (0 0 1) zone axis is displayed in Fig. 4(c). The interplanar distances, calculated from the highly magnified image, were determined to be 3.0 Å, 2.9 Å and 3.5 Å which in turn corresponds to the (0 2 0), (3 1 0) and (3 0 0) planes, respectively and is in consensus with the results observed from the SAED pattern in Fig. 4(a). Moreover, these values are comparable to those calculated theoretically from the olivine structure of $LiFePO_4$ obtained using crystallographic simulation, as is evidenced from Fig. 4(c).

This result is particularly interesting in understanding the ion-transport kinetics of nanocrystalline $LiFePO_4$ because it suggests that plate-type nanoparticles with crystal growth orientations in specific directions can be synthesized using the solvothermal method. Ceder and coworkers reported that Li-ion hopping along the b axis is permissible in the olivine structure, because of the low activation barrier along that direction [31]. Chen et al. reported that lithium is extracted at narrow disordered transition zones on the *ac* crystal surface, and that the existence of particles with large ac faces can therefore improve rate capabilities [32]. From this standpoint of view, $LiFePO_4$ synthesized in the form of nanoplates with crystal growth orientations along the a–c plane can be considered to be more beneficial for Li-ion mobility along 1D [0 1 0] direction. However, the olivine nanoplates synthesized in the present study appear to indicate growth along the a–b plane and thereby possibly retard-

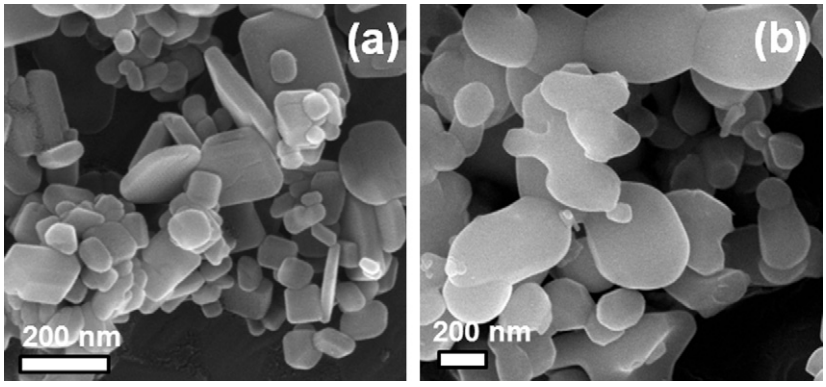

Fig. 3. FE-SEM images of the $LiFePO_4$ samples synthesized by (a) solvothermal and (b) solid state reaction.

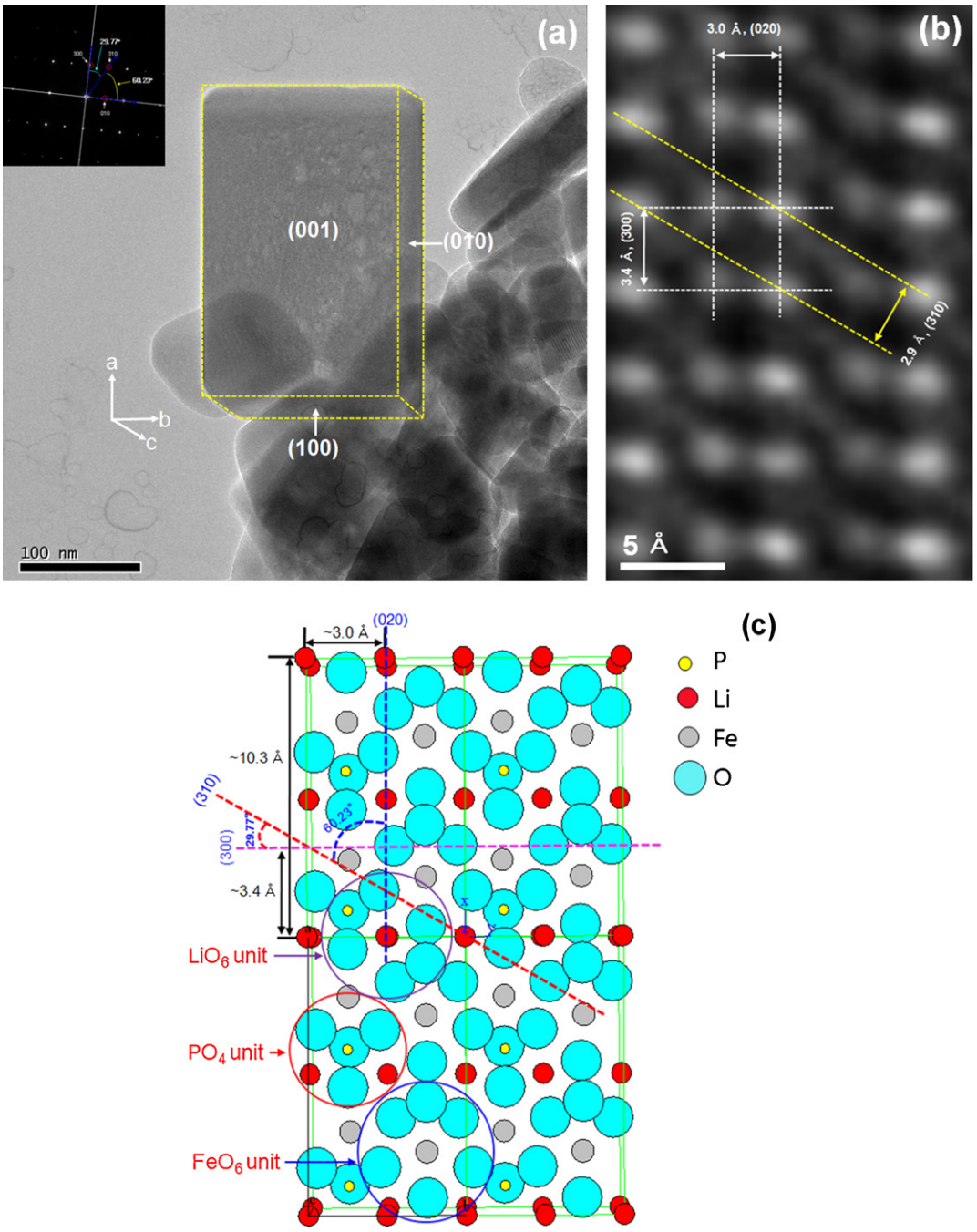

Fig. 4. The field emission-TEM images of the nanoplate $LiFePO_4$; (a) a low magnification image with the selected area electron diffraction pattern, (b) the magnified high-resolution image, and (c) crystallographic simulation of the $LiFePO_4$ structure.

ing the Li-ion motion in the ideally favored [0 1 0] direction along the a–c plane. Therefore, these results indicate that limitations in the electrochemical performances of the solvothermal-based olivine can be anticipated though the present investigation certainly sheds more light on the growth characteristics of nano-plate type $LiFePO_4$ synthesized at low temperatures.

Fig. 5 shows the voltage profiles during 1st charging–discharging and cyclabilities of the $LiFePO_4$ prepared by solvothermal and solid state reaction at a current density of 0.1 mA/cm^2 in the voltage range 2.5–4.2 V. Plate $LiFePO_4$ exhibited lower initial discharge capacity (138 mA h/g) than that of the sample synthesized by solid state method probably arising from the limitations of the kinetic dynamics pertaining to the Li-ion in the present sample. However, nanoplate $LiFePO_4$ indicates stable capacity retention after 20 cycles, while cyclability of the $LiFePO_4$ prepared by solid state reaction decreases steadily during 50 cycles in Fig. 5(b). This result clearly indicates that though the initial capacities of the nano-plate sample appear not to be satisfactory, the performance during extended cycling is comparable to that of the high-temperature solid-state sample thus suggesting a well ordered structure with considerable electrochemical stability.

Fig. 6 shows the rate performances of the $LiFePO_4$ electrodes prepared by solvothermal and solid state reaction at 0.5–16 C-rates after cycling three times at each rate. Even though nanoplate $LiFePO_4$ shows lower discharge capacity at 0.5 C-rate, it appears to be considerably better in its rate performance for progressing C-rates when compared to that obtained for $LiFePO_4$ when synthesized by the solid state method. The better rate performance in the

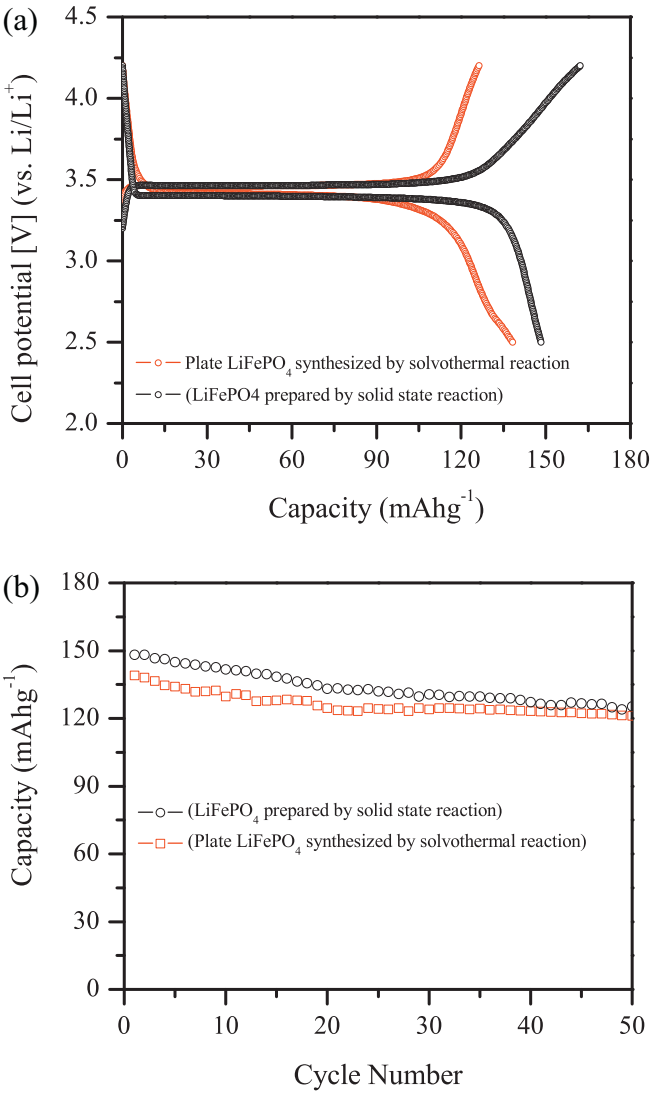

Fig. 5. Electrochemical performances of the $LiFePO_4$ samples synthesized by solvothermal and solid state reaction; (a) initial charge/discharge curves of the $LiFePO_4$ sample under a current density 0.1 mA/cm^2 within the voltage range of 2.5–4.2 V and (b) the capacity retention rate of $LiFePO_4$ during 50 cycles.

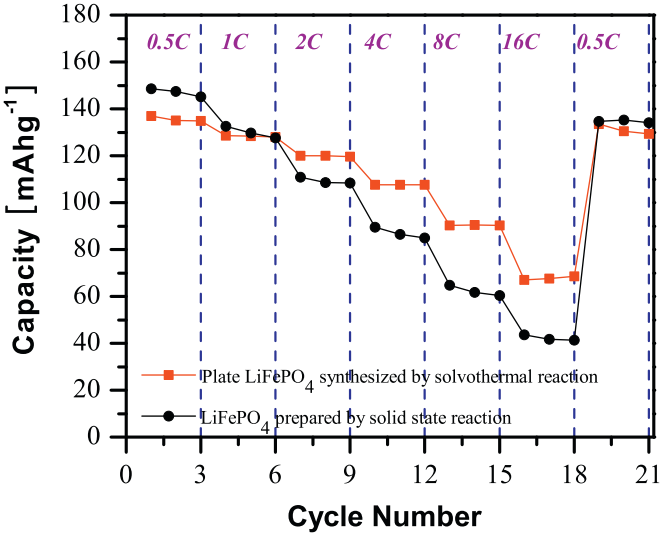

Fig. 6. The C-rate performances of the $LiFePO_4$ samples prepared by solvothermal and solid state reaction at 0.5 C–16 C-rates after cycling three times at each rate.

synthesized nanoplate $LiFePO_4$ at enhanced C-rates is most probably due to the contribution from nanoparticles [27] whereas the diffusion limit caused by larger particles in the solid state sample, as shown in SEM images, is the most feasible reason for the slump in its electrochemical performance.

Generally, the primary reason for capacity loss is mainly associated with the constraints in large particles due to their apparently lower surface area and the diffusion limit of lithium ions through the decreasing $LiFePO_4/FePO_4$ interface. Therefore, in our previous study, we focused on producing nanoelectrodes with minute particle sizes and uniform size distribution [27] that exhibited good capacity and high rate performance though they appear to suffer from limitations of low tap densities for practical applications. Hence, in the present study, we successfully synthesized plate-type nano-olivine with apparently larger sizes in the range 100–300 nm using a solution based technique, to tailor the particle-sizes of olivine nanocrystals [33]. Further, this aspect provides the possibility to synthesize plate-type particles with desired crystal growth orientations which ultimately is sure to enhance electrochemical performances and tap densities.

It remains crucial to develop cheaper and simpler synthetic procedures to obtain nano-sized particles with high crystalline traits for successful commercialization. Therefore, it is worth noting that the solvothermal process performed in the present study enables the synthesis of highly crystalline $LiFePO_4$ nanoplates at low temperatures while it was only possible to obtain poorly crystalline or amorphous nano-olivine in the same polyol medium at similar temperatures using the polyol refluxing technique. However, the synthesized nanoplate based $LiFePO_4$ cathode shows fair electrochemical performance, due to the short path length of lithium ions from the core of the particles to the surface. Nevertheless, some modification is further required to increase the tap density and rate capability before this material can be used in commercial electrodes, which we believe, could be achieved by developing nanoplate $LiFePO_4$ possessing minute dimensions of thickness along its "*b*"-axis to facilitate the fast diffusion of lithium ions. In this regard, although the nano-sized particles with a size of 200–300 nm synthesized by the solvothermal method with a plate morphology did not show ideal crystal-growth promoting the facile movement of Li-ion in the [0 1 0] direction, the results tend to suggest that it would be possible to control the morphology of the nanoplates with regard to the a–c plane and ultimately attain suitable tap densities for commercial applications. Therefore, further studies are required to monitor the morphological features and understand the correlation between particle morphology and rate capability systematically through an extensive set of experiments.

4. Conclusions

$LiFePO_4$ nanocrystals were synthesized by the solvothermal method in a polyol medium (DEG) with the concerned precursors maintained at 200 °C for 16 h. Synchrotron powder XRD analysis confirmed that all peaks could be indexed to a pure orthorhombic, olivine-type structure (space group: Pnma) with no trace of impurities. XPS analysis revealed the divalent state of Fe in the $LiFePO_4$ sample prepared by low temperature solvothermal reaction and thereby confirmed the formation of phase-pure olivine. The obtained nanocrystalline $LiFePO_4$ particles mainly showed plate-type morphologies with an average length, width and thickness of 250, 200 and 20 nm, respectively. The TEM analysis showed that the $LiFePO_4$ nanoplates grew in the a–b plane, though growth orientation along the crystallographic a–c plane ideally favors Li-ion motion. Plate-type $LiFePO_4$ indicated initial discharge capacity of 138 mA h/g and maintained stable capacity retentions from 20

to 50 cycles. When compared to $LiFePO_4$ synthesized by the solid state method, solvothermal or nanoplate-type $LiFePO_4$ appeared to exhibit considerably better rate performance at enhanced C-rates most probably due to the contribution from nano-dimensional particles with large surface areas.

Acknowledgements

This research was supported by WCU (World Class University) program through the Korea Science and Engineering Foundation funded by the Ministry of Education, Science and Technology (grant number; R32-20074).

References

[1] A.K. Padhi, K.S. Nanjundaswamy, J.B. Goodenough, J. Electrochem. Soc. 144 (1997) 1188.
[2] N. Ravert, Y. Chouinard, J.F. Magnan, S. Besner, M. Gauthier, M. Armand, J. Power Sources 97–98 (2001) 503.
[3] Y. Cui, X. Zhao, R. Guo, J. Alloys Compd. 490 (2010) 236.
[4] Y.D. Li, S.X. Zhao, C.W. Nan, B.H. Li, J. Alloys Compd. 509 (2011) 957.
[5] H. Huang, S.C. Yin, L.F. Nazar, Electrochem. Solid-State Lett. 14 (2001) A170.
[6] Y.H. Huang, J.B. Goodenough, Chem. Mater. 20 (2008) 7237.
[7] Y. Ding, Y. Jiang, F. Xu, J. Yin, H. Ren, Q. Zhuo, Z. Long, P. Zhang, Electrochem. Commun. 12 (2010) 10.
[8] S.Y. Chung, J.T. Bloking, Y.M. Chiang, Nat. Mater. 1 (2002) 123.
[9] H. Liu, Q. Cao, L.J. Fu, C. Li, Y.P. Wu, H.Q. Wu, Electrochem. Commun. 8 (2006) 1553.
[10] Y. Wang, Y. Yang, X. Hu, Y. Yang, H. Shao, J. Alloys Compd. 481 (2009) 590.
[11] A.Y. Shenouda, H.K. Liu, J. Alloys Compd. 477 (2009) 498.
[12] A. Yamada, S. Nishimura, H. Koizumi, R. Kanno, S. Seki, Y. Kobayashi, H. Miyashiro, J. Dodd, R. Yazami, B. Fultz, Mater. Res. Soc. Symp. Proc. 972 (2006) AA13.
[13] C. Delacourt, P. Poizot, S. Levasseur, C. Masquelier, Electrochem. Solid-State Lett. 9 (2006) A352.
[14] K. Dokko, S. Koizumi, H. Nakano, K. Kanamura, J. Mater. Chem. 17 (2007) 4803.
[15] B. Ellis, W.H. Kan, W.R.M. Makahnouk, L.F. Nazar, J. Mater. Chem. 17 (2007) 3248.
[16] A.V. Murugan, T. Muraliganth, A. Manthiram, Electrochem. Commun. 10 (2008) 903.
[17] K. Saravanan, P. Balaya, M.V. Reddy, B.V.R. Chowdari, J.J. Vittal, J. Mater. Chem. 19 (2008) 605.
[18] D. Kim, J. Lim, E. Choi, J. Gim, V. Mathew, Y. Paik, H. Jung, W. Lee, D. Ahn, S. Paek, J. Kim, Surf. Rev. Lett. 17 (2010) 111.
[19] A. Yamada, S.C. Chung, K. Hinokuma, J. Electrochem. Soc. 148 (2001) A224.
[20] S. Yang, P. Zavalij, M.S. Whittingham, Electrochem. Commun. 3 (2001) 505.
[21] J. Yang, J.J. Xu, Electrochem. Solid-State Lett. 7 (2004) A515.
[22] G. Arnold, J. Garche, R. Hemmer, S. Strobele, C. Volger, M. Wohlffahrt-Mehrens, J. Power Sources 119–121 (2003) 247.
[23] S. Franger, F.L. Cras, C. Bourbon, H. Rouault, J. Power Sources 119–121 (2003) 252.
[24] K.S. Park, J.T. Son, H.T. Chung, S.J. Kim, C.H. Lee, K.T. Kang, H.G. Kim, Solid-State Commun. 129 (2004) 311.
[25] F. Croce, A.D. Epifanio, J. Hassoun, A. Deptual, T. Olczac, Electrochem. Solid-State Lett. 5 (2002) A47.
[26] H. Yang, X.L. Wu, M.H. Cao, Y.G. Guo, J. Phys. Chem. C 113 (2009) 3345.
[27] D.H. Kim, J. Kim, Electrochem. Solid-State Lett. 9 (2006) A439.
[28] D.H. Kim, J.S. Im, J.W. Kang, E.J. Kim, H.Y. Ahn, J. Kim, J. Nanosci. Nanotechnol. 7 (2007) 3949.
[29] J. Chen, M.S. Whittingham, Electrochem. Commun. 8 (2006) 855.
[30] Y.H. Rho, L.F. Nazar, L. Perry, D. Ryan, J. Electrochem. Soc. 154 (2007) A283.
[31] D. Morgan, A. Van der Ven, G. Ceder, Electrochem. Solid-State Lett. 7 (2004) A30.
[32] G. Chen, X. Song, T.J. Richardson, Electrochem. Solid-State Lett. 9 (2006) A295.
[33] D.H. Kim, J. Kim, J. Phys. Chem. Solids 68 (2007) 734.